

in all $(1/\sqrt{Z})^6$ and summations and integrations over three independent momenta contributing

$$\frac{1}{Z^3} \sum_h \int dh_0 \sim (\sqrt{Z})^3.$$

The amplitude therefore behaves as

$$W^4(\sqrt{Z})^3/(\sqrt{Z})^6 \sim \sqrt{Z} \text{ if } W \sim \sqrt{Z}$$

as in Bopp's theory. By similar considerations one finds that the amplitude corresponding to a Feynman diagram of any order behaves as \sqrt{Z} . The corresponding differential scattering cross-section $d\sigma/d\Omega$ is found to behave as $1/Z^2$. This behaviour becomes somewhat milder if the amplitude is a

chain of diagrams, because then [using (4.5) as an example] the scattering cross-section has to be divided by e^2 and so behaves as $1/e^2 Z^2 \sim (\ln Z)^{-2}$. We see therefore that the Z -dependence of W which was chosen³ to ensure a finite, noninfinite mass of the quasiparticles results in vanishing cross-sections at least in the limit $Z \rightarrow \infty$. This may best be understood by observing¹⁴ that in a continuum theory this procedure corresponds to the replacement $g \rightarrow g/\Lambda^2$, where Λ is the cutoff.

The author is indebted to Professor F. BOPP for suggesting this investigation and to him and Dr. E. G. WEIDEMANN and M. LÖWER for numerous discussions.

¹³ H. UMEZAWA, Quantum Field Theory, North-Holland Publ. Co., Amsterdam 1956, pp. 41, 118.

¹⁴ M. LÖWER, Dr.-thesis, University of München 1970.

Impurity-induced and Second Order Raman Spectra of NaCl Crystals Doped with Different Ag^+ Concentrations

W. MÖLLER and R. KAISER

Physik-Department der Technischen Hochschule München, Germany

(Z. Naturforsch. 25 a, 1024—1029 [1970]; received 24 April 1970)

Raman spectra of NaCl crystals doped with Ag^+ ions up to 3.5 mol% have been measured in 4 scattering geometries. In the impurity induced part of the E_g - and F_{2g} -spectra the strongest peaks are located at 85 and 171 cm^{-1} . Their intensities increase proportional to the silver concentration. The second order Raman spectrum on the other hand appears to be independent of the Ag^+ content. The spectra are fully explained by theory and by the assumption of Ag^+ pairs.

Introduction

Besides well known methods like optical absorption and thermal conductivity spontaneous Raman scattering recently has proven as a useful tool for investigating the influence of point imperfections on the vibrations of the host lattice. If such imperfections are introduced into a cubic alkali halide crystal the translational symmetry of the lattice is disturbed. Then not only the two-phonon Raman spectrum which is alone allowed in the pure crystal

but also one phonon scattering may be expected. This scattering is in general characteristic of both the host lattice and the particular imperfections.

In recent years the influence of various kinds of lattice imperfections such as atomic impurities¹⁻⁴, diatomic and molecular impurities⁵⁻⁹ as well as F-centers^{10, 11} has been investigated in alkali halide crystals. First order Raman effect could be clearly established in KBr crystals, doped with Cl^- ions¹, in NaCl doped with Ag^+ ³ and in three potassium halides doped with Ti^{+4} .

¹ I. P. HURRELL, S. P. S. PORTO, T. C. DAMEN, and S. MASCARENHAS, Phys. Letters 26 A, 194 [1968].

² R. KAISER and P. MÖCKEL, Phys. Letters 25 A, 747 [1967].

³ R. KAISER and W. MÖLLER, Phys. Letters 28 A, 619 [1969].

⁴ R. T. HARLEY, J. B. PAGE, JR., and C. T. WALKER, Phys. Rev. Lett. 23, 922 [1969].

⁵ M. I. W. SHEPARD, A. R. EVANS, and D. B. FITCHEN, Phys. Letters 27 A, 171 [1968].

⁶ W. HOLZER, W. F. MURPHY, H. J. BERNSTEIN, and J. ROLFE, J. Mol. Spectr. 26, 543 [1968].

⁷ W. R. FENNER and M. V. KLEIN, Light Scattering Spectra of Solids, ed. by G. B. WRIGHT, New York 1969 (Proc.

Int. Conf. on Light Scattering Spectra of Solids, New York University, New York, Sept. 1968), p. 497.

⁸ R. H. CALLENDER and P. S. PERSHAN, Light Scattering Spectra 1969, see. Ref. 7, p. 505.

⁹ W. C. HOLTON and M. DEWIT, Sol. State Commun. 7, 1099 [1969].

¹⁰ J. M. WORLOCK and S. P. S. PORTO, Phys. Rev. Letters 15, 697 [1965].

¹¹ B. FRITZ, Localized Excitations in Solids, edited by R. F. WALLIS, New York 1968, p. 497 (Proc. First Intern. Conference on Localized Excitations in Solids, Univ. of California, Irvine, Sept. 1967).



Raman experiments with doped alkali halides supply information which cannot be obtained from the IR absorption or the thermal conductivity¹². While for the point group O_h of the alkali halides only the odd vibration of T_{1u} is IR active, the even vibrations of A_{1g} , E_g and F_{2g} type are Raman active. The Raman active vibrations can be investigated separately by measuring the crystal in the appropriate scattering geometry. Thus, in alkali halides IR and Raman experiments complement each other. Finally the thermal conductivity as an integral effect is sensitive to odd and even vibrations. Here the individual vibrations cannot be observed. It is extremely difficult, if possible at all, to analyse the temperature dependent thermal conductivity in terms of special odd or even phonon vibrations.

In the system NaCl—AgCl a strong resonant absorption of type T_{1u} caused by the Ag^+ impurity has been found in the IR at 50.5 cm^{-1} (290°K)¹³. On the other hand, the Raman spectra of these crystals contain the E_g , F_{2g} modes and vibrations by impurity pairs as already reported by us previously in a short note¹⁴.

It is the aim of this work to investigate the influence of the Ag^+ concentration on these E_g and F_{2g} modes and on the two-phonon processes.

Experimental

A Coherent Radiation Argon-ion laser operating with 0.9 W in the 4880 Å line, a grating double monochromator and a phase sensitive detection system were used. The laser beam was focussed into the entrance slit of the spectrometer. The spectral resolution is about 3 cm^{-1} .

The Ag^+ concentration of the samples was determined by neutron activation analysis. This method gives the Ag^+ concentration in the system NaCl—AgCl in good agreement with colorimetric¹⁵ and chemical^{15a} analyses.

The crystals of rectangular shape are 30–50 mm long and $10 \times 10\text{ mm}$ wide.

Scattering Geometry

The laser beam was incident parallel to the longest axis (Z) of the crystal, the X - and Y -axis coincide with the two shorter axes of the crystal.

The four terms containing the X , Y , Z -axes used in the following text and the figures indicate, according to common praxis¹ the direction and the polarization of the incident and scattered light as follows: first term: direction of the incident light; second term (first term in paranthesis): polarization of the incident light; third term (second term in paranthesis): polarization of the scattered light; fourth term: direction of the scattered light.

The point group for an atomic impurity in the NaCl crystal is O_h . In this case only even vibrations of the types A_{1g} , E_g and F_{2g} are Raman active¹⁶. The crystals are measured in three geometries denoted by α , β , γ . Though the three arrangements (α , β , γ) are sufficient for the complete determination of the three vibrations A_{1g} , E_g and F_{2g} a fourth geometry δ was also measured in order to check the other three geometries.

The tensor components a^2 , b^2 , d^2 of the O_h point group¹⁶ are proportional to the scattering intensities I in the appropriate geometry. The F_{2g} vibration, corresponding to the tensor component d^2 can be obtained in the $Z(Y, Z)X$ arrangement (γ), while for the E_g vibrations with the tensor component $3b^2$ the $XY(XY, XY)Z$ geometry (β) was selected (\overline{XY} indicating $\overline{110}$, XY indicating 110 direction). The $Z(Y, Y)X$ arrangement (α) permits the sum of the A_{1g} and E_g vibrations with the tensor components $a^2 + 4b^2$ from which the A_{1g} vibration can be obtained by subtracting the b^2 component of the E_g vibration, determined according to the (β) geometry^{16, 17}. The fourth geometry $XY(\overline{XY}, \overline{XY})Z$ (δ) gives the sum of the A_{1g} , E_g and F_{2g} vibrations (tensor components $a^2 + b^2 + d^2$).

Results

Types of Vibrations

The Raman spectra of the NaCl crystal with the highest Ag^+ concentration (3.5 mol-%) in the four geometries α , β , γ , δ are presented in Fig. 1. The tensor components d^2 for the F_{2g} (γ) and b^2 for the E_g (β) vibrations are obtained directly, the tensor component a^2 for the A_{1g} vibrations by the following subtractions of the scattering intensities

¹² M. V. KLEIN, in: Physics of Color Centers, Chapt. 7, ed. by W. B. FOWLER, Academic Press, London 1968.

¹³ R. WEBER and F. SIEBERT, Z. Physik **213**, 273 [1968] and private communication.

¹⁴ W. MÖLLER, R. KAISER, and H. BILZ, Phys. Letters **32 A**, 171 [1970].

¹⁵ K. FUSSGAENGER, W. MARTIENSEN, and H. BILZ, Phys. Stat. Sol. **12**, 383 [1965].

^{15a} We are grateful to Prof. A. WEISS, Universität München, for chemical analyses of our crystals.

¹⁶ R. LOUDON, Adv. Physics **13**, 423 [1964].

¹⁷ M. KRAUZMAN, C. R. Acad. Sci. Paris **266 B**, 186 [1968].

$$I_{\alpha} - 4/3 I_{\beta} \quad \text{or} \quad I_{\delta} - 1/3 I_{\beta} - I_{\gamma}.$$

The measured intensities in the four geometries according to Fig. 1 are found to be consistent with each other within a few percent.

In Fig. 2 the scattering spectra in the same geometries as in Fig. 1, but for the pure NaCl crystal measured under the same conditions as the doped crystals in Fig. 1, are presented. These spectra are in agreement with the results of KRAUZMAN¹⁸. A comparison of the Raman scattering of the doped NaCl crystals (Fig. 1) with the scattering of the pure NaCl crystal (Fig. 2) shows that a number of additional scattering peaks with very strong vibrations at 85 cm⁻¹ (E_g) and 171 cm⁻¹ (F_{2g}) arises in the doped specimen. The frequencies and the types of vibrations found by us experimentally are listed in the first column of Table 1. The experimentally determined wave numbers may be in error by about ± 2 cm⁻¹.

Obviously the peaks at 47, 85/87, 112, 135/137, 171 are the same as the peaks at 58, 88, 117, 140, 177 cm⁻¹ reported by us earlier in the unpolarized Raman spectrum³ with an equipment permitting only limited accuracy particularly at small frequency shifts.

Concentration Dependence of the Impurity Induced and Second Order Raman Spectrum

F_{2g} Spectrum

The F_{2g} spectrum showing the largest number of features has been measured in NaCl crystals with various silver concentrations (Fig. 3). The following results should be noted:

With increasing Ag⁺ content strong Raman scattering arises below $\cong 200$ cm⁻¹ with peaks at 87, 135 and 171 cm⁻¹. At 171 cm⁻¹ the scattering in the crystal with the highest Ag⁺ concentration (3.5 mol-% Ag⁺) according to Fig. 3 d becomes approximately four times stronger than the most prominent peak in the second order spectrum of the pure crystal (Fig. 3 a) at 236 cm⁻¹. The scattering of the crystal with 3.5 mol-% Ag⁺ at 171 cm⁻¹ (Fig. 3 d) is more than 30 times stronger than the scattering of the pure crystal at the same frequency (Fig. 3 a).

The spectra of the doped crystals below $\cong 100$ cm⁻¹ consist of impurity induced contributions and of second order components. This second order scattering becomes more and more negligible the higher the impurity induced spectrum grows. For comparison the second order scattering contribution is indicated (dashed line) in the Figs. 3 b – d.

In Fig. 4 the scattering intensity of the strongest F_{2g} vibration at 171 cm⁻¹ is plotted against the Ag⁺ concentration of the NaCl crystals. It turns out that the impurity induced Raman scattering is proportional to the Ag⁺ concentration.

Since the impurity induced Raman scattering extends to no more than $\cong 200$ cm⁻¹ the second order Raman spectrum, which is the only one present in the pure NaCl crystals, can be observed in all the Ag⁺ doped crystals above $\cong 200$ cm⁻¹. It can be seen from Fig. 3 a – d that the second order Raman scattering of the Ag⁺ doped crystals remains of the same magnitude as the scattering of the pure crystal. Therefore, the second order Raman spectrum appears to be independent of the Ag⁺ impurity concentration.

E_g Spectrum

Similarly to the F_{2g} spectrum the E_g scattering increases with the Ag⁺ concentration as can be seen from Fig. 5. According to Fig. 5, curve d, the strongest peak in the E_g spectrum at 85 cm⁻¹ in the crystal with the highest silver content (3.5 mol-% Ag⁺) is about 50 times stronger than the scattering of the pure crystal at the same frequency (Fig. 5, curve a).

Also in the case of the strong E_g vibration at 85 cm⁻¹ the scattering intensity plotted versus Ag⁺ concentration shows a linear relationship (Fig. 4).

Comparison with Theory and Conclusions

A number of papers have been published dealing with response functions and different models of imperfect crystals^{19–21}. The calculations of BENEDEK and NARDELLI¹⁹ were made on the basis of Hardy's deformation dipole model for the host lattice dynamics under the assumption that the non central interaction can be neglected. These authors give the projected density of states for the even symmetry modes

¹⁸ M. KRAUZMAN, Light Scattering Spectra, 1969, see Ref. 7, p. 109.

¹⁹ G. BENEDEK and G. F. NARDELLI, J. Chem. Phys. **48**, 5242 [1968].

²⁰ M. F. MACDONALD, M. V. KLEIN, and T. P. MARTIN, Phys. Rev. **177**, 1292 [1969].

²¹ For further references see Ref. 19.

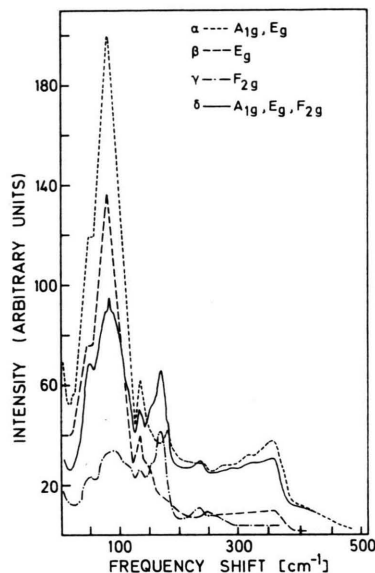


Fig. 1. Raman spectrum of NaCl with 3.5 mol-% Ag^+ , measured in four scattering geometries:

- α Z(Y, Y)X;
 β XY(XY, XY)Z;
 γ Z(Y, Z)X;
 δ XY(XY, XY)Z.

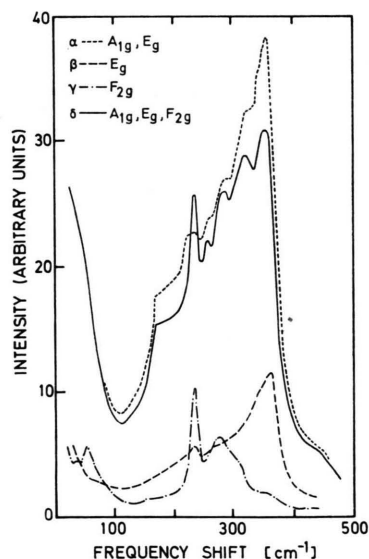


Fig. 2. Raman spectrum of a pure NaCl crystal measured in four scattering geometries:

- α Z(Y, Y)X;
 β XY(XY, XY)Z;
 γ Z(Y, Z)X;
 δ XY(XY, XY)Z.

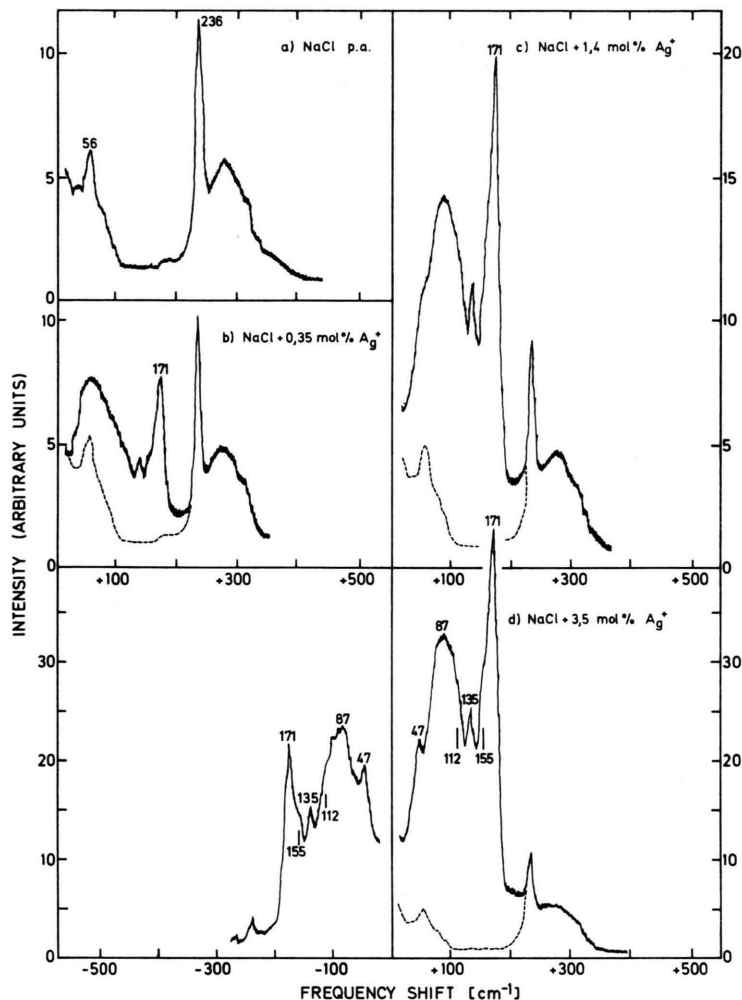


Fig. 3 a-d. Raman scattering intensities of the F_{2g} vibration (γ -geometry) of a pure NaCl crystal (a) and 3 crystals with different Ag^+ content (b-d), dashed lines in Fig. 3 b-d indicate second order scattering of pure NaCl (Fig. 3 a).

in NaCl. Their density of states is calculated for various values of the fractional change in force constant by the impurity. The change of the force constant brought about by the Ag^+ impurity in NaCl is calculated in Ref. ¹⁹ from the IR absorption of the system NaCl - AgCl at 52.5 cm^{-1} (4.2°K).

According to these calculations the density of states for the F_{2g} vibrations of the NaCl crystal shows peaks at 117, 140, 155 and 174 cm^{-1} . In addition the density of states in the NaCl lattice, perturbed by the Ag^+ impurity, results in a strong E_g vibration peaking at 87 cm^{-1} and a smaller peak at 137 cm^{-1} . Since the Raman scattering tensor is

proportional to the density of states the frequencies according to the calculations of Benedek and Nardelli are listed in the second column of Table 1.

Comparing the calculated scattering peaks with our experimental data the following points should be noted:

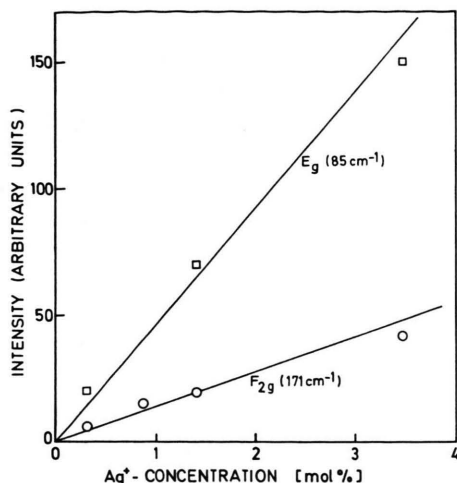


Fig. 4. Concentration dependence of the scattering intensities of the E_g - (measured at 85 cm^{-1} in β -geometry) and F_{2g} - (measured at 171 cm^{-1} in γ -geometry) vibrations.

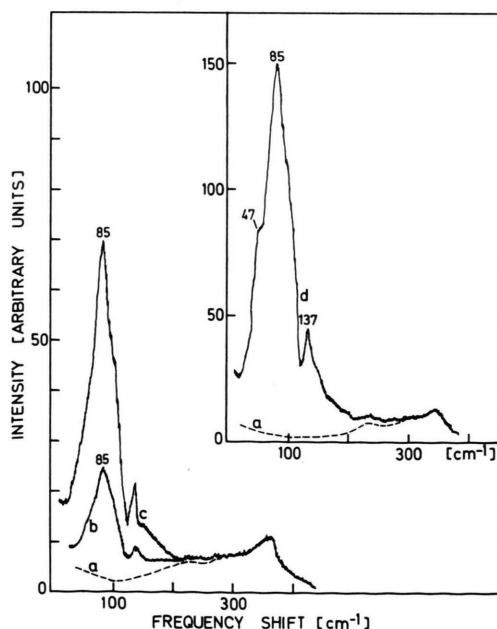


Fig. 5. Raman scattering intensities of the E_g vibration (β -geometry) for pure NaCl (curve a) and NaCl crystals containing 0.35 mol-% Ag^+ (curve b); 1.4 mol-% Ag^+ (curve c); 3.5 mol-% Ag^+ (curve d).

1. In the E_g spectrum our experimental peaks at 85 and 135 cm^{-1} agree well with theoretical predictions¹⁹. The E_g vibration at 85 cm^{-1} is also in good agreement with the frequency of this vibration suggested by thermal conductivity measurements^{22, 23}.

2. In the F_{2g} spectrum four experimental peaks at 112 , 135 , 155 and 171 are well accounted for by theory.

3. The measured A_{1g} contribution is so small that it remains within the limits of error. Thus the predicted peak at 124 cm^{-1} of the A_{1g} vibration could not be found experimentally. In this connection it should be pointed out that in KCl and KJ halides doped with Ti^{4+} also no A_{1g} vibration has been observed. Very small phonon scattering from A_{1g} modes has also been concluded from the analysis of thermal conductivity measurements^{22, 23}.

4. The scattering in the F_{2g} spectrum around 87 cm^{-1} of medium intensity is not expected on theoretical grounds. From the calculations only a small feature shows up in the F_{2g} spectrum¹⁹ around 80 cm^{-1} . But due to the finite angle of the scattering beam in the proper geometry for the F_{2g} vibrations a certain percentage from the very strong E_g vibration at about the same frequency (85 cm^{-1} , Figs. 1 and 5) will also appear in the F_{2g} spectrum.

5. The scattering peaks at 47 cm^{-1} which were not explained by the theory of BENEDÉK and NARDELLI¹⁹, appear only in crystals with a high silver content. We found that both the scattering intensity at 47 cm^{-1} and the absorption constant of the A^* band in the UV which has been attributed to Ag^+ pairs¹⁵ are proportional to the square of the Ag^+ concentration. Therefore, the peak at 47 cm^{-1} was assigned by us to a Ag^+ pair vibration¹⁴. This Ag^+ pair frequency in which the impurity is vibrating coincides aside from a small shift to lower wave numbers essentially with the odd, IR active T_{1u} mode at 50.5 cm^{-1} (290°K)¹³.

The calculation of the frequency ω_p of this Ag^+ pair vibration is strictly valid only for a vibration of F_{2g} type. It is possible that the calculated pair frequency of E_g type turns out to be slightly different from ω_p of F_{2g} type. Within experimental accuracy, however, no difference in the low frequency

²² R. C. CALDWELL and M. V. KLEIN, Phys. Rev. **158**, 851 [1967].

²³ F. C. BAUMANN and R. O. POHL, Phys. Rev. **163**, 843 [1967].

peaks at 47 cm^{-1} was found in the E_g and F_{2g} vibrations.

It must be mentioned that only the positions but not the intensities of the observed and calculated peaks have been compared. An additional comparison of the intensities might be particularly useful if calculations based on different theoretical models were available. Then the various models could be judged how well they fit the experimental data. However, at present only the calculations of Benedek and Nardelli are available.

In conclusion it can be stated that the experimentally determined peaks in the scattering spectrum are fully explained on theoretical grounds.

We thank Prof. K. DRANSFELD for his permanent interest in this work. Thanks are due to Prof. H. BILZ and Dr. D. STRAUCH for discussion and to the Deutsche Forschungsgemeinschaft for financial support.

	Experiment cm^{-1}	Theory ¹⁹ cm^{-1}	Ag ⁺ pair frequency ¹⁴ cm^{-1}
A_{1g}	—	124	
	47		a
E_g	85 (s)	87	
	137 (m)	137	
	47 (w)		47.5
	87 (m)	(80), ^b	
F_{2g}	112 (w)	117	
	135 (m)	140	
	155 (w)	155	
	171 (s)	174	

a The pair frequency of type E_g may be slightly different from $\omega_P = 47.5\text{ cm}^{-1}$ (F_{2g} -type), see text.

b Strong peak at 85 cm^{-1} in E_g geometry, see text.

Table 1. Position of the peaks in the Raman spectra (1. column: Experiment) and in the density of states (2. column: Theory). The calculated Ag⁺ pair frequency is listed in the 3. column. The observed Raman intensities are denoted by s (strong), m (medium) and w (weak).

Microwave Absorption Spectra of AlF, GaF, InF, and TlF

J. HOEFT, F. J. LOVAS, E. TIEMANN, and T. TÖRRING

II. Physikalisches Institut der Freien Universität Berlin

(Z. Naturforsch. **25 a**, 1029—1035 [1970]; received 4 May 1970)

Observation of various rotational transitions of four Group IIIa monofluoride allowed the Dunham coefficients Y_{01} , Y_{11} , Y_{21} and Y_{12} to be determined. From the hyperfine structure of the AlF, GaF and InF spectra, the nuclear electric quadrupole coupling constants, $e q_V Q$, and spin-rotation coupling constant, c_I , were obtained for several vibrational states, v :

$$\begin{aligned} e q_V Q(^{27}\text{Al } ^{19}\text{F}) &= -37.75(8) + 0.44(8) (v+1/2) \text{ MHz}, \\ e q_V Q(^{69}\text{Ga } ^{19}\text{F}) &= -107.07(8) + 1.09(7) (v+1/2) \text{ MHz}, \\ e q_V Q(^{71}\text{Ga } ^{19}\text{F}) &= -67.46(8) + 0.68(7) (v+1/2) \text{ MHz}, \\ e q_V Q(^{115}\text{In } ^{19}\text{F}) &= -727.06(20) + 6.64(20) (v+1/2) \text{ MHz}. \end{aligned}$$

Stark effect measurements on GaF and InF in the ground vibrational state resulted in the following electric dipole moments:

$$\begin{aligned} ^{69}\text{Ga } ^{19}\text{F}: & \quad |\bar{\mu}_0| = 2.45(5) \text{ D}, \\ ^{115}\text{In } ^{19}\text{F}: & \quad |\bar{\mu}_0| = 3.40(7) \text{ D}. \end{aligned}$$

Introduction

Microwave absorption studies of the Group IIIa monofluorides have resulted in improved rotational and hyperfine structure constants for AlF and InF and the first observation of the GaF spectrum. Previously, only the $v=0$ and 1 spectra of AlF¹ and InF² were reported, leaving the rather large Y_{21}

($=\gamma_e$) rotational constant unknown, so that the reported Y_{01} and Y_{11} rotational constants are somewhat erroneous.

An additional goal of this work was to obtain more accurate hyperfine interaction constants, $e q_V Q$ and c_I , for the Al, Ga and In nuclei and to determine the molecular electric dipole moments of GaF and InF. The rotational constants³, magnetic hyper-

Sonderdruckanforderungen an Professor Dr. J. HOEFT, II. Physikalisches Institut der Freien Universität Berlin, D-1000 Berlin 33, Boltzmannstr. 20.

¹ DAVID R. LIDE, JR., J. Chem. Phys. **38**, 2027 [1963]; **42**, 1013 [1965].

² F. J. LOVAS and T. TÖRRING, Z. Naturforsch. **24 a**, 634 [1969].

³ H. G. FITZKY, Z. Physik **151**, 351 [1958]. — R. K. RITCHIE and H. LEW, Can. J. Phys. **43**, 1701 [1965]. — A. H. BARRETT and M. MANDEL, Phys. Rev. **109**, 1572 [1958].